


The topographical anatomy of the posterior auricular artery: a computed tomography angiography analysis with implications for reconstructive surgery

Mateusz Trzeciak¹, Patryk Ostrowski^{1, 2}, Michał Bonczar^{1, 2}, Alicia del Carmen Yika¹, Kinga Gładys¹, Ahmed Elsaftawy³, Wadim Wojciechowski⁴, Mateusz Koziej^{1, 2}, Jerzy Walocha^{1, 2} , Artur Pasternak¹

¹Department of Anatomy, Jagiellonian University Medical College, Kraków, Poland

²Youthoria, Youth Research Organization, Kraków, Poland

³Department of Plastic and Hand Surgery, Trzebnica, Poland

⁴Department of Radiology, Jagiellonian University Medical College, Kraków, Poland

[Received: 16 August 2023; Accepted: 23 October 2023; Early publication date: 8 November 2023]

Background: The anatomy of the posterior auricular artery (PAA) is highly variable and relevant in various plastic and reconstructive procedures.

Materials and methods: The results of 55 consecutive patients who underwent head and neck computed tomography angiography (CTA) were analysed. A total of 78 hemifaces were evaluated. The analysis has been performed in 19 categories.

Results: Median PAA length was found to be 47.59 mm (LQ = 32.75; HQ = 56.16). The median PAA diameter (at its origin) was established at 2.55 mm (LQ = 2.29; HQ = 2.90). Moreover, the median PAA cross-sectional area (at its origin) was set to be 3.22 mm (LQ = 2.49; HQ = 4.13). Sexual dimorphism regarding all of the measured parameters was also evaluated. Statistically significant differences ($p \leq 0.05$) were found in 13 of the measured categories.

Conclusions: The present study demonstrated the complete anatomy of the PAA. The most frequent origin of the said artery was from the ECA, and its mean length was 45.07 mm; which did not differ significantly between males and females ($p > 0.05$). Moreover, we have provided surgeons with tools to localize this artery pre- and intraoperatively using simple landmarks, namely the apex of the mastoid process and the centre of the external acoustic meatus. The exact position of the origin of the PAA was also demonstrated by a heat map of the auricular region. Our findings have the potential to assist surgeons in developing a mental visualization of the arterial anatomy of the retroauricular region. This visualization can be instrumental in precisely identifying the location of the PAA during reconstructive surgeries, thereby minimizing complications and enhancing surgical outcomes. (Folia Morphol 2024; 83, 3: 647–655)

Keywords: posterior auricular artery, head and neck surgery, retroauricular, anatomy

Address for correspondence: Mateusz Trzeciak, Department of Anatomy, Jagiellonian University Medical College, ul. Mikołaja Kopernika 12, 33–332 Kraków, Poland; e-mail: trzeciak.mateusz6@gmail.com

This article is available in open access under Creative Common Attribution-Non-Commercial-No Derivatives 4.0 International (CC BY-NC-ND 4.0) license, allowing to download articles and share them with others as long as they credit the authors and the publisher, but without permission to change them in any way or use them commercially.

INTRODUCTION

The posterior auricular artery (PAA) is a branch of the external carotid artery (ECA), typically found as its final preterminal branch. It travels upward in a posterior direction, running between the external acoustic meatus and the mastoid process. Its primary role is to supply blood to various structures in the surrounding regions, including the adjacent muscles, the parotid gland, the facial nerve, as well as structures within the temporal bone, auricle, and scalp [8]. Several studies have highlighted the variability in the general anatomy of the PAA and other branches of the ECA [10, 11, 16], including its morphometric characteristics such as length and diameter [14]. In fact, the length of the PAA exhibits significant variability, which lead to the development of a novel classification system by Tokugawa et al. [14] solely based on these length variations. However, there is a lack of studies that have specifically examined the topographical anatomy of the PAA, something that would be incredibly useful for both plastic and reconstructive surgeons and neurosurgeons.

The retroauricular tissues have been used for a long time for various reconstructive procedures, and are mainly supplied by the PAA. Reconstructive flaps that rely on the blood supply provided by the said artery have been employed in plastic and reconstructive surgery since the 1960s and were first introduced by Washio [15]. Since then, numerous studies have presented the use of retroauricular tissues for various reconstructions, especially of the ear, with satisfactory results [2, 3, 12, 13]. Moreover, the PAA has also been used as a novel landmark for the identification of the facial nerve [5, 6], as well as a donor artery for cerebral revascularization surgeries [9]. However, the variable anatomy of the PAA may pose problems for surgeons performing the aforementioned procedures. Therefore, the core aim of the current study was to generate a heat map, pinpointing the precise position of the PAA. Our results may help surgeons to create a mental map of the arterial anatomy of the retroauricular region, which can aid in accurately locating the PAA during reconstructive procedures, reducing complications, and improving surgical outcomes.

MATERIALS AND METHODS

Approval of the bioethical committee

The research protocol was submitted for evaluation and approved by the Jagiellonian University Bioethical Committee, Cracow, Poland (1072.6120.51.2022).

The study was carried out according to the allowed criteria during the next stages.

Study group

The results of 55 consecutive patients who underwent head and neck computed tomography angiography (CTA) in the Department of Radiology of the Jagiellonian University Medical College, Cracow, Poland, were evaluated in July 2022. Each CTA was evaluated bilaterally; therefore, a total of 110 hemifaces were initially evaluated. Exclusion criteria were established as follows: (1) head, neck, or/and thoracic trauma affecting the course and/or the morphometry of the PAA and/or its close anatomical area, (2) significant artifacts that prevented accurate and precise imaging and/or measurement of the PAA and/or its close anatomical area, (3) low quality and illegible images, and (4) significant lack of filling the whole arterial system with contrast. If only a part of the CTA was affected by any of the defects mentioned above, without interference with the contralateral side, the other PAA was independently evaluated. The great majority ($n = 32$) of the excluded hemifaces were not analysed due to significant artifacts. The remaining two were excluded due to bias prevention as the images were low-quality. Finally, a total of 76 hemifaces met the inclusion criteria.

Results acquisition

All head and neck CTA were performed on a 128-slice scanner CT (Philips Ingenuity CT, Philips Healthcare). The main CT imaging parameters were the following: collimation/increase: 0.625/0.3 mm; tube current: 120 mAs; field of view: 210 mm; matrix size: 512 × 512.

All patients received intravenous administration of contrast material at a dose of 1 mL/kg (standard dose). A non-ionic contrast medium (CM) containing 350 mg of iodine per mL was used (Jowersol 741 mg/mL, Optiray®, Guerbet, France). The acquisition of CT data was initiated using a real-time bolus tracking technique (Philips Healthcare) with the region of interest (ROI) placed in the ascending aorta. CM was injected intravenously using a power injector at a flow rate of 5 mL/s. This was immediately followed by an injection of 40 mL of saline solution at the same flow rate. Following injection of CM and saline, image acquisition was automatically started with a 2 s delay when the attenuation trigger value reached a threshold of 120 Hounsfield units (HU). Scanning

was performed in the caudocranial direction. The CTA examination was started at the level of the aortic arch up to the circle of Willis.

The CTAs were analysed on a dedicated workstation in the Anatomical Department of Jagiellonian University Medical College, Cracow, Poland. To ensure the highest possible quality of the visualizations and measurements and minimize potential bias, Materialise Mimics Medical version 21.0 software (Materialise NV, Leuven, Belgium) software was used. 3-dimensional (3D) reconstructions of each scan were developed, employing a set of settings, severally adjusted to each scan. A volume rendering opacity range oscillated from 25 to 75 HU for the lower limit and up to 135 HU for a higher limit. The range was individually adjusted to each TT after a visual investigation.

Evaluation and measurements

At the start of each examination, each PAA has been completely visualized. Subsequently, a set of measurements was enrolled in each PAA by two independent researchers separately, and a mean was established, taking into account both results. All measurements were rounded to two decimal places. Morphometric features of the SA and/or its associated anatomical area were measured/assessed in 19 categories: (1) PAA length; (2) PAA diameter (at its origin); (3) PAA cross-sectional area (at its origin); (4) PAA branching angle [deg]; (5) ECA diameter at the PAA origin; (6) ECA cross-sectional area at the PAA origin; (7) CCA diameter (just before bifurcation); (8) CAA cross-sectional area (just before bifurcation); (9) MA diameter (at its origin); (10) MA cross-sectional area (at its origin); (11) OA diameter (at its origin); (12) OA cross-sectional area (at its origin); (13) FA diameter (at its origin); (14) FA cross-sectional area (at its origin); (15) distance from the origin of the OA to the origin of the PAA (over the surface of the ECA); (16) distance from the origin of the FA to the origin of the PAA (over the surface of the ECA); (17) distance from the origin of the PAA to the origin of the MA (over the surface of the ECA); (18) distance from the PAA to the mastoid process (vertical plane); (19) distance from the centre of the external acoustic meatus to the PAA (horizontal plane). The results were established in millimetres (mm/mm²). The measured parameters are presented in Figures 1 and 2.

Furthermore, a set of measurements was taken in order to establish an anatomical heat map of the occurrence of the origin of the PAA. On the basis of these

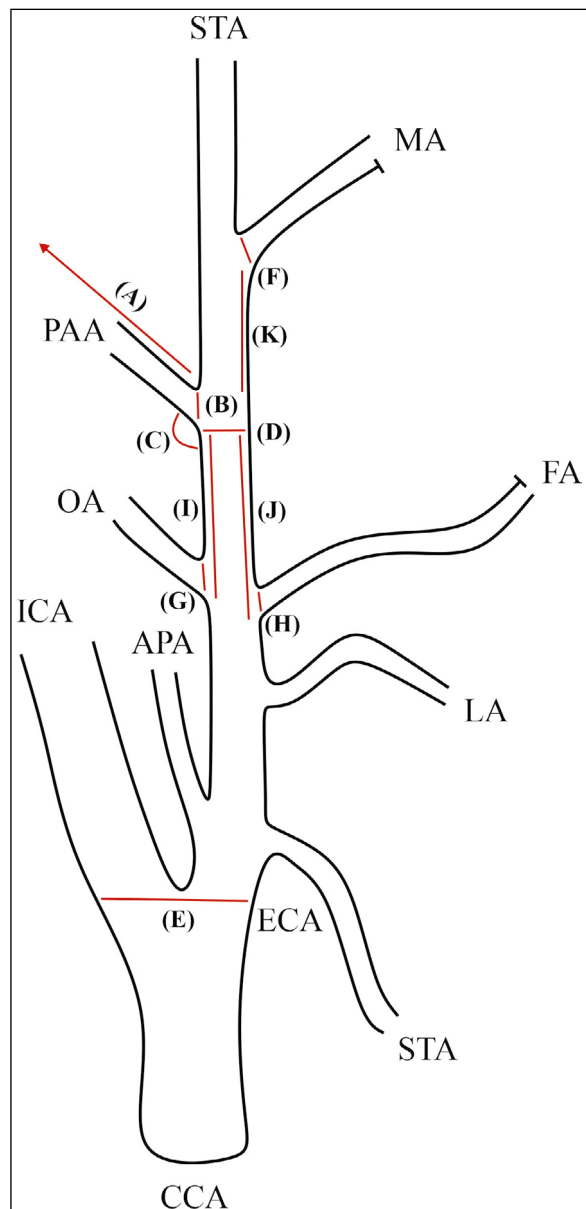


Figure 1. Scheme presenting the measurement taken during the present study. A — PAA length; B — PAA diameter and cross-sectional area (at its origin); C — PAA branching angle; D — ECA diameter and cross-sectional area (at its origin); E — CCA diameter and cross sectional area (just before bifurcation); F — MA diameter and cross-sectional area (at its origin); G — OA diameter and cross-sectional artery (at its origin); H — FA diameter and cross-sectional area (at its origin); I — distance from the origin of the OA to the origin of the PAA; J — distance from the origin of the FA to the origin of the PAA; K — distance from the origin of the PAA to the origin of the MA. APA — ascending pharyngeal artery; CCA — common carotid artery; ECA — external carotid artery; FA — facial artery; ICA — internal carotid artery; LA — lingual artery; MA — maxillary artery; OA — occipital artery; PAA — posterior auricular artery; STA — superior thyroid artery; STA — superficial temporal artery.

measurements, a unified triangle was established. Thereafter, the shortest distances from the origins of

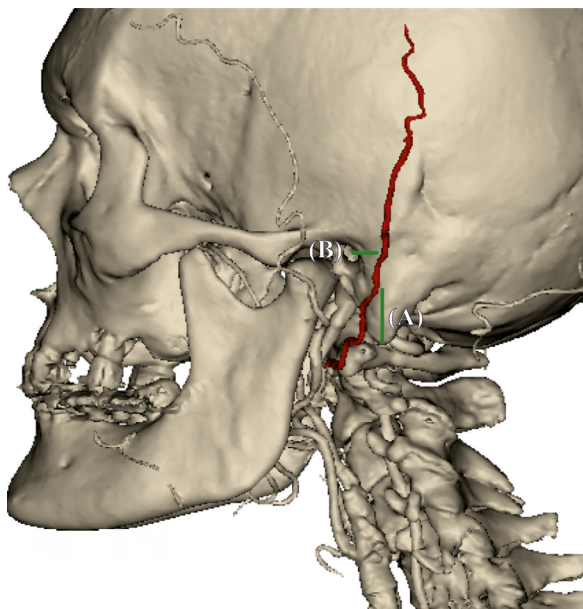


Figure 2. Illustration presenting the measurements taken during the present study. A — distance from the PAA to the mastoid process (vertical plane); B — distance from the centre of the external acoustic meatus to the PAA (horizontal plane). PAA — posterior auricular artery.

each of the SA to the sides of the triangle were measured. All measurements were taken at a fixed angle in order to minimize potential bias. Furthermore, the points of origin of each PAA were scaled and applied to the heatmap with respect to the enrolled measurements. Heat maps of the origin of the SA from the lateral points of view are presented in Figures 3 and 4.

Statistical analysis

Statistical analysis was performed with STATISTICA v13.1 (StatSoft Inc., Tulsa, OK, USA). The frequency and percentages presented qualitative features. The Shapiro-Wilk test was used to assess the normal distribution. Quantitative characteristics were presented by medians and upper and lower quartiles (UQ, LQ), as well as means and standard deviation (SD), depending on the verified normality of the data. Statistical significance was defined as $p < 0.05$. Mann-Whitney and Wilcoxon signed-rank tests were used to establish potential differences between groups. The Spearman rank correlation coefficient was used to determine possible correlations between the parameters.

RESULTS

The results of the present study were established based on a total of 76 hemifaces. Out of those, 34 were female patients (44.7%), whereas 42 were male

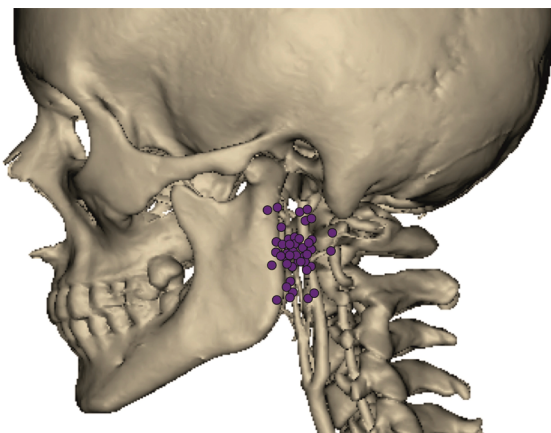


Figure 3. Heatmap of the origin of the posterior auricular artery — view on the left side.

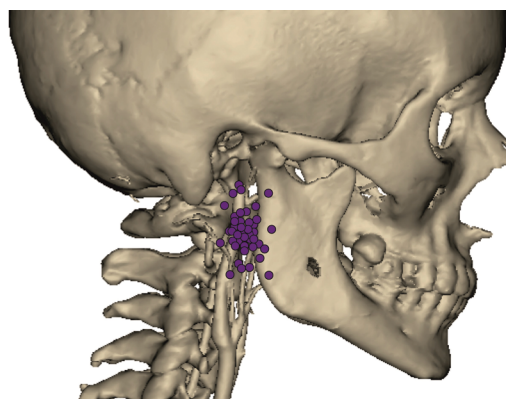


Figure 4. Heatmap of the origin of the posterior auricular artery (PAA) — view on the right side.

patients (55.3%). Left and right sides were established in equal amounts, 38 each. PAA was found to originate from ECA in 66 of the cases (86.8%), whereas from OA only in 8 of the cases (10.5%). Detailed general results can be found in Table 1.

The median PAA length was found to be 47.59 mm (LQ = 32.75; HQ = 56.16). The median PAA diameter (at its origin) was established at 2.55 mm (LQ = 2.29; HQ = 2.90). The median PAA cross-sectional area (at its origin) was set to be 3.22 mm (LQ = 2.49; HQ = 4.13). The median branching angle of the PAA was found to be 68.09 degrees (LQ = 44.51; HQ = 87.59). The median distance from the origin of the OA to the origin of the PAA (over the surface of the ECA) was found to be 26.03 mm (LQ = 22.02; HQ = 31.90). The median distance from the origin of the FA to the origin of the PAA (over the surface of the ECA) was established at 26.83 mm (LQ = 21.66; HQ = 34.31). The median distance from the origin of the PAA to

the origin of the MA (over the surface of the ECA) was set to be 21.12 mm (LQ = 16.15; HQ = 23.93). The median distance from the PAA to the mastoid process in the vertical plane was set to be 27.08 mm

(LQ = 21.57; HQ = 29.94). The median distance from the centre of the external acoustic meatus to the PAA horizontal plane was established at 15.10 mm (LQ = 11.14; HQ = 18.34). Detailed results in all categories can be found in Table 2.

Table 1. Qualitative results of the data analysis.

Category	N	Percentage [%]
Patients' sex		
Females	34	44.7
Males	42	55.3
Patients' side		
Left	38	50.0
Right	38	50.0
PAA origin artery		
ECA	66	86.8
OA	8	10.5
STA	1	1.3
ICA	1	1.3

ECA — external carotid artery; ICA — internal carotid artery; OA — occipital artery; PAA — posterior auricular artery; STA — superficial temporal artery.

Furthermore, sexual dimorphism regarding all of the measured parameters has been evaluated. Statistically significant differences ($p \leq 0.05$) were found in 13 of the measured categories: PAA diameter; PAA cross-sectional area; ECA diameter at the PAA origin; ECA cross-sectional area at the PAA origin; CCA diameter; CCA cross-sectional area; MA diameter; OA diameter; OA cross-sectional area; FA diameter; FA cross-sectional area; distance from the origin of the FA to the origin of the PAA; distance from the PAA to the mastoid process. Detailed results regarding sexual dimorphism are presented in Table 3.

Subsequently, differences between patients' sides and correlations between parameters and patients' age were studied. However, there were no statistical differences ($p > 0.05$) between patients' sides in

Table 2. Overall results of the measurements. The results were established in millimetres [mm/mm²].

Category	Median	LQ	HQ	Minimum	Maximum	Mean	SD
PAA length	47.59	32.75	56.16	15.24	84.78	45.07	15.74
PAA diameter (at its origin)	2.55	2.29	2.90	1.42	3.73	2.54	0.46
PAA cross-sectional area (at its origin)	3.22	2.49	4.13	1.25	5.97	3.28	1.12
PAA branching angle [deg]	67.09	44.51	87.59	23.23	145.41	69.84	29.37
ECA diameter at the PAA origin	4.23	3.79	4.74	2.57	5.68	4.28	0.64
ECA cross-sectional area at the PAA origin	10.26	8.23	12.22	3.94	16.88	10.43	2.83
CCA diameter (just before bifurcation)	8.09	7.37	8.82	4.84	11.78	8.16	1.31
CCA cross-sectional area (just before bifurcation)	41.88	35.12	50.67	13.80	77.26	43.03	12.40
MA diameter (at its origin)	3.35	3.13	3.58	1.76	4.50	3.31	0.51
MA cross-sectional area (at its origin)	6.25	5.28	7.20	1.34	11.22	6.24	1.76
OA diameter (at its origin)	2.87	2.48	3.16	1.51	5.08	2.83	0.63
OA cross-sectional area (at its origin)	4.24	3.22	5.62	1.13	8.46	4.36	1.61
FA diameter (at its origin)	3.24	2.89	3.66	1.99	5.00	3.27	0.61
FA cross-sectional area (at its origin)	6.03	4.52	7.36	2.19	14.17	6.17	2.22
Distance from the origin of the OA to the origin of the PAA (over the surface of the ECA)	26.03	22.02	31.90	5.48	53.96	27.21	10.24
Distance from the origin of the FA to the origin of the PAA (over the surface of the ECA)	26.83	21.66	34.31	11.12	60.37	28.91	9.49
Distance from the origin of the PAA to the origin of the MA (over the surface of the ECA)	21.12	16.15	23.93	3.28	30.07	19.73	5.63
Distance from the PAA to the mastoid process (vertical plane)	27.08	21.57	29.94	12.76	36.89	25.75	5.98
Distance from the PAA to the centre of the external acoustic meatus (horizontal plane)	15.10	11.14	18.34	8.23	20.11	14.55	4.33

CCA — common carotid artery; ECA — external carotid artery; FA — facial artery; HQ — higher quartile; LQ — lower quartile; MA — maxillary artery; OA — occipital artery; PAA — posterior auricular artery; SD — standard deviation.

Table 3. Results of the measurements with respect to the patients' sex. The results were established in millimetres [mm/mm²].

Category	Sex	Median	LQ	HQ	Minimum	Maximum	Mean	SD	P-value
PAA length	Females	45.33	29.24	50.51	15.24	68.57	42.07	14.60	0.16
	Males	49.62	34.64	58.87	16.04	84.78	47.24	16.36	
PAA diameter (at its origin)	Females	2.47	2.19	2.68	1.50	3.54	2.45	0.45	0.04
	Males	2.60	2.48	2.98	1.42	3.73	2.62	0.47	
PAA cross-sectional area (at its origin)	Females	2.67	2.04	3.67	1.25	5.97	2.88	1.14	0.00
	Males	3.67	3.07	4.26	1.57	5.38	3.60	1.02	
PAA branching angle [deg]	Females	61.90	41.64	77.89	23.23	125.40	63.49	27.97	0.08
	Males	72.46	56.19	93.74	23.31	145.41	75.09	29.80	
ECA diameter at the PAA origin	Females	3.88	3.71	4.30	2.57	5.42	4.03	0.68	0.00
	Males	4.45	4.18	4.90	3.53	5.68	4.48	0.53	
ECA cross-sectional area at the PAA origin	Females	8.25	7.21	9.75	3.94	16.88	9.07	2.98	0.00
	Males	11.26	10.16	12.72	7.44	16.77	11.53	2.19	
CCA diameter (just before bifurcation)	Females	7.55	7.08	8.51	5.46	10.55	7.74	1.14	0.01
	Males	8.43	7.74	9.31	4.84	11.78	8.51	1.35	
CCA cross-sectional area (just before bifurcation)	Females	37.85	33.04	47.20	20.11	68.70	39.75	11.09	0.02
	Males	44.20	37.92	52.84	13.80	77.26	45.69	12.88	
MA diameter (at its origin)	Females	3.23	2.78	3.53	1.76	4.19	3.16	0.57	0.05
	Males	3.48	3.15	3.65	2.49	4.50	3.44	0.42	
MA cross-sectional area (at its origin)	Females	6.23	4.49	7.18	1.34	9.12	5.93	1.92	0.44
	Males	6.28	5.62	7.22	3.22	11.22	6.49	1.61	
OA diameter (at its origin)	Females	2.61	2.29	2.92	1.51	3.85	2.54	0.53	0.00
	Males	3.04	2.64	3.43	2.03	5.08	3.05	0.63	
OA cross-sectional area (at its origin)	Females	3.50	2.96	4.25	1.13	6.51	3.60	1.29	0.00
	Males	4.97	3.86	5.78	2.31	8.46	4.96	1.60	
FA diameter (at its origin)	Females	3.02	2.71	3.27	1.99	3.82	2.94	0.49	0.00
	Males	3.59	3.16	3.90	2.29	5.00	3.54	0.57	
FA cross-sectional area (at its origin)	Females	4.92	3.88	6.02	2.19	7.36	4.93	1.44	0.00
	Males	6.98	5.82	8.33	3.32	14.17	7.18	2.25	
Distance from the origin of the OA to the origin of the PAA (over the surface of the ECA)	Females	23.94	18.47	32.93	6.93	53.96	26.02	11.82	0.23
	Males	27.08	23.33	31.42	5.48	50.41	28.18	8.81	
Distance from the origin of the FA to the origin of the PAA (over the surface of the ECA)	Females	23.92	20.15	30.50	11.12	60.37	26.79	10.51	0.02
	Males	29.49	25.07	34.89	17.94	53.22	30.57	8.36	
Distance from the origin of the PAA to the origin of the MA (over the surface of the ECA)	Females	20.77	16.05	23.95	3.28	30.07	19.83	5.70	1.00
	Males	21.26	16.21	23.91	7.09	29.50	19.65	5.64	
Distance from the PAA to the mastoid process (vertical plane)	Females	24.87	20.32	28.27	13.36	36.89	24.28	5.72	0.02
	Males	28.90	23.72	30.93	12.76	36.72	26.95	5.97	
Distance from the PAA to the centre of the external acoustic meatus (horizontal plane)	Females	14.30	9.43	15.20	7.42	18.34	14.12	4.15	0.27
	Males	15.03	10.01	15.77	9.33	21.44	15.14	4.44	

CCA — common carotid artery; ECA — external carotid artery; FA — facial artery; HQ — higher quartile; LQ — lower quartile; MA — maxillary artery; OA — occipital artery; PAA — posterior auricular artery; SD — standard deviation.

any of the parameters. Furthermore, no statistically significant correlation between any of the parameters and patients' age was found.

DISCUSSION

The anatomy and the blood supply area, or angiogram, of the PAA, have been discussed in the

literature. The morphometric properties of the said artery have been analysed extensively by Tokugawa et al. [14], in a study based on 234 patients that underwent conventional cerebral angiographies. In the study, they mainly focused on the length of the PAA, because of the potential implications of this vessel in cerebral revascularizations. Due to the high variability of the lengths of the PAAs, a classification system that consisted of four types was created: Type A, the PAA terminates between the origin and the centre of the external acoustic canal (15.1%); Type B, the PAA terminates between the origin and the top of the helix of the ear (34.9%); Type C; the PAA terminates between the top of the helix and the vertex (48.8%); and Type D, the PAA reaches up to the vertex (1.2%). The authors of the aforementioned study further discussed that if a patient has a Type D PAA, the artery could be used as a donor artery for revascularization surgery. However, they did not provide any specific numerical data regarding the morphometric properties of the said vessel. This has been supplemented by the current study; the mean length of the PAA was 45.07 mm; with a range between 15.24 mm and 84.78 mm. Our results further demonstrate the variability of the length of this artery. However, the length did not differ between males and females significantly ($p > 0.05$). Moreover, the mean diameter of the PAA was found to be 2.54 mm. Interestingly, it was quite similar to the diameter of the OA (2.83); however, it was smaller than the MA (3.31 mm) and the FA (3.27 mm). Furthermore, the results of the current study demonstrate that the most common origin of the PAA is from the ECA (86.8%), as described in major anatomical textbooks. However, the said artery originated relatively frequently from the OA (10.5%), and very rarely from the STA (1.3%) and ICA (1.3%). These variations have also been described by the pioneering work of Buntaro Adachi [1], *Das Arteriensystem der Japaner*, and by Lippert and Pabst [4] in *Arterial Variations in Man*. The data presented in the current study can provide physicians with deeper knowledge regarding the appropriate anatomy for revascularization surgeries, in cases where the typical arteries used are not feasible.

More recent studies have focused more on the blood supply area, or the angiosome, of the PAA. This was first done by McKinnon et al. [7] in 1999, in a study consisting of eight fresh cadavers. In the study, they concluded that the PAA had a consistent vascular anatomy and angiosome. Moreover, it was

stated that the cutaneous distribution of the said vessel suggests that a large pedicled or island flap based on the PAA may be raised safely as a myocutaneous or myofasciocutaneous flap. In a more recent study conducted by Gómez Díaz and Cruz Sánchez [2], it was stated that the PAA irrigated an area of the retroauricular skin and fascia of 10.7 cm length \times 7.07 cm wide, which was equivalent to 60.44 cm². They concluded that a fascia or fasciocutaneous flap from the retroauricular area within the dimension that they presented would be safe for reconstructions of the ear. Studies demonstrating the morphometric properties and the angiosome of the PAA are highly relevant for reconstructive surgeries. However, no study has yet analysed the topography of this vessel. Moreover, there are no methods of localizing the PAA pre- or intra-operatively. Therefore, the present study provided topographical relationships between the artery and nearby anatomical landmarks, namely the apex of the mastoid process and the centre of the external acoustic meatus. The mean measurements between the PAA and these landmarks are presented in Figure 2. Moreover, a heat map showing the exact origin of the said artery from the lateral view was created (Fig. 3, 4). This data can be of incredible use when harvesting any reconstructive flap pedicled on the PAA because it can aid surgeons in creating a mental map of the vasculature of the retroauricular region intraoperatively by using simple anatomical landmarks mentioned earlier. Moreover, due to the high degree of variability in both the morphometric and topographic characteristics of this vessel, the authors of the present study strongly advise surgeons to analyse the arterial anatomy of the retroauricular area preoperatively with CTAs and potentially Doppler ultrasonography in each patient individually.

The PAA has been proposed as a novel anatomical landmark for the identification of the facial nerve. Liu et al. [5, 6] analysed the relationship between these two structures due to the high facial nerve dysfunction rate during parotidectomies. In their cadaveric study, it was stated that the trunk of the facial nerve crossed the artery inferior to the stylomastoid foramen, and the nerve could be precisely identified by tracing the PAA proximally. Moreover, the authors of the said study found that the distance from the cross point of the PAA and the facial nerve to the external meatal cartilage was 5.2 ± 0.2 mm [6]. Later, the same authors performed a clinical study where this technique was put to use. In the study, the PAA could

be exposed in 28 out of 31 (90.3%) patients during parotidectomy, and the facial nerve trunk could be identified by the guide of the artery in all cases [5]. Most importantly, no iatrogenic damage to the facial nerve occurred; proving the reliability of the PAA as the ideal landmark for early identification of the facial nerve. Unfortunately, the relationship between these two structures could not be analysed in the present study because our results are based on angiographies. However, the tools presented in our study may help with the initial localization of the PAA prior to its subsequent dissection proximally in order to find the trunk of the facial nerve.

The present study has several limitations. Radiological imaging only allows one to evaluate haemodynamically efficient arteries. Therefore, this can be a relatively significant source of bias when assessing anatomical variations of the PAA and other arterial entities. Taking into account that the more patients are examined in a study, the more accurate it is, the results of the present article may be burdened with a potential bias as the number of studied hemifaces was only 78. Especially burdened might be the results regarding the sexual dimorphism in which the groups were even smaller. Although not without limitations, our study attempts to thoroughly analyse the anatomy of the PAA using methods that meet the requirements of evidence-based anatomy.

CONCLUSIONS

The present study demonstrated the complete anatomy of the PAA. The most frequent origin of the said artery was from the ECA, and its mean length was 45.07 mm; which did not differ between males and females significantly ($p > 0.05$). Moreover, we have provided surgeons with tools to localize this artery pre- and intraoperatively using simple landmarks, namely the apex of the mastoid process and the centre of the external acoustic meatus. The exact position of the origin of the PAA was also demonstrated by a heat map of the auricular region. Our findings have the potential to assist surgeons in developing a mental visualization of the arterial anatomy of the retroauricular region. This visualization can be instrumental in precisely identifying the location of the PAA during reconstructive surgeries, thereby minimizing complications and enhancing surgical outcomes.

ARTICLE INFORMATION AND DECLARATIONS

Data availability statement

The data that support the findings of this study are available from the corresponding author, upon reasonable request.

Ethics statement

The research protocol was submitted for evaluation and approved by the Jagiellonian University Bioethical Committee, Cracow, Poland (1072.6120.51.2022). The study was carried out according to the allowed criteria during the next stages.

Author contributions

Mateusz Trzeciak: methodology, measurements, writing, heatmaps, figures, tables. **Patryk Ostrowski:** methodology, writing, literature. **Michał Bonczar:** methodology, statistical analysis, writing. **Alicia del Carmen Yika:** measurements, data selection. **Kinga Gładys:** measurements, data selection. **Ahmed Elsaftawy:** writing, literature. **Wadim Wojciechowski:** data selection, writing. **Mateusz Koziej:** statistical analysis, writing. **Jerzy Walocha:** writing, tables. **Artur Pasternak:** writing, methodology.

Funding

The authors received no financial support for the research, authorship, and/or publication of this article.

Conflict of interest

The authors declare no potential conflicts of interest with respect to the research, authorship, and/or publication of this article.

REFERENCES

1. Adachi B, Hasebe K. *Das Arteriensystem der Japaner*. Kenkyusha, Tokyo 1928.
2. Gómez Díaz OJ, Cruz Sánchez MD. Anatomical and Clinical Study of the Posterior Auricular Artery Angiosome: In Search of a Rescue Tool for Ear Reconstruction. *Plast Reconstr Surg Glob Open*. 2016; 4(12): e1165, doi: [10.1097/GOX.0000000000001165](https://doi.org/10.1097/GOX.0000000000001165), indexed in Pubmed: [28293515](https://pubmed.ncbi.nlm.nih.gov/28293515/).
3. Jadhav C, Rawlins J. Extended posterior auricular artery flap for temporo-parietal scalp defect in previously irradiated scalp. *J Craniofac Surg*. 2016; 27(3): e261–e262, doi: [10.1097/SCS.0000000000002492](https://doi.org/10.1097/SCS.0000000000002492), indexed in Pubmed: [27035598](https://pubmed.ncbi.nlm.nih.gov/27035598/).
4. Lippert H, Pabst R. *Arterial variations in man classification and frequency*. J.F. Bergmann-Verlag, Munich 1985.

5. Liu M, Tong L, Xu M, et al. Posterior auricular artery as a novel anatomic landmark for identification of the facial nerve: A clinical study. *Laryngoscope Investig Otolaryngol.* 2022; 7(5): 1441–1447, doi: [10.1002/lio2.894](https://doi.org/10.1002/lio2.894), indexed in Pubmed: [36258872](https://pubmed.ncbi.nlm.nih.gov/36258872/).
6. Liu M, Wang SJ, Benet A, et al. Posterior auricular artery as a novel anatomic landmark for identification of the facial nerve: A cadaveric study. *Head Neck.* 2018; 40(7): 1461–1465, doi: [10.1002/hed.25127](https://doi.org/10.1002/hed.25127), indexed in Pubmed: [29566447](https://pubmed.ncbi.nlm.nih.gov/29566447/).
7. McKinnon BJ, Wall MP, Karakla DW. The vascular anatomy and angiosome of the posterior auricular artery. A cadaver study. *Arch Facial Plast Surg.* 1999; 1(2): 101–104, doi: [10.1001/archfaci.1.2.101](https://doi.org/10.1001/archfaci.1.2.101), indexed in Pubmed: [10937086](https://pubmed.ncbi.nlm.nih.gov/10937086/).
8. Moore KL, Dalley AF, Agur A. *Clinically oriented anatomy* (8th ed). Lippincott Williams and Wilkins, Philadelphia 2017.
9. Niwa R, Kimura T, Ichi S. Occipital artery-anterior cerebral artery bypass with posterior auricular artery-middle cerebral artery bypass for stenosis of the internal carotid artery bifurcation. *Br J Neurosurg.* 2021; 35(6): 792–795, doi: [10.1080/02688697.2019.1620919](https://doi.org/10.1080/02688697.2019.1620919), indexed in Pubmed: [31144536](https://pubmed.ncbi.nlm.nih.gov/31144536/).
10. Ostrowski P, Bonczar M, Yika AD, et al. The occipital-vertebral anastomosis revisited. *Folia Morphol.* 2023; 82(3): 615–623, doi: [10.5603/FM.a2022.0101](https://doi.org/10.5603/FM.a2022.0101), indexed in Pubmed: [36472395](https://pubmed.ncbi.nlm.nih.gov/36472395/).
11. Ostrowski P, Szczepanek E, Niemczyk K, et al. A 3D map of the lingual artery — the perfect tool for transoral robotic surgeries on the base of tongue. *Head Neck.* 2023; 45(4): 872–881, doi: [10.1002/hed.27303](https://doi.org/10.1002/hed.27303), indexed in Pubmed: [36807690](https://pubmed.ncbi.nlm.nih.gov/36807690/).
12. Pierrefeu A, Bonnafous S, Gagnieur P, et al. Posterior auricular artery helix root free flap-part II: clinical application. *Int J Oral Maxillofac Surg.* 2022; 51(5): 632–636, doi: [10.1016/j.ijom.2021.10.005](https://doi.org/10.1016/j.ijom.2021.10.005), indexed in Pubmed: [34716073](https://pubmed.ncbi.nlm.nih.gov/34716073/).
13. Sharma RK, Pandey SK. Extended posterior auricular artery flap for coverage of a large temporo-parietal defect. *J Plast Reconstr Aesthet Surg.* 2010; 63(11): e775–e778, doi: [10.1016/j.bjps.2010.06.022](https://doi.org/10.1016/j.bjps.2010.06.022), indexed in Pubmed: [20692214](https://pubmed.ncbi.nlm.nih.gov/20692214/).
14. Tokugawa J, Cho N, Suzuki H, et al. Novel classification of the posterior auricular artery based on angiographical appearance. *PLoS One.* 2015; 10(6): e0128723, doi: [10.1371/journal.pone.0128723](https://doi.org/10.1371/journal.pone.0128723), indexed in Pubmed: [26030595](https://pubmed.ncbi.nlm.nih.gov/26030595/).
15. Washio H. Retroauricular temporal flap. *Plast Reconstr Surg.* 1969; 43(2): 162–166, doi: [10.1097/00006534-196902000-00009](https://doi.org/10.1097/00006534-196902000-00009), indexed in Pubmed: [4885510](https://pubmed.ncbi.nlm.nih.gov/4885510/).
16. Żytkowski A, Tubbs R, Iwanaga J, et al. Anatomical normality and variability: Historical perspective and methodological considerations. *Transl Res Anat.* 2021; 23: 100105, doi: [10.1016/j.tria.2020.100105](https://doi.org/10.1016/j.tria.2020.100105).